



An optimized network for drought prediction using satellite images

Bhagvat D Jadhav ^{a,*}, Pravin Marotrao Ghate ^a, Prabhakar Narasappa Kota ^b,
Shankar Dattatray Chavan ^c, Pravin Balaso Chopade ^b

^a Department of Electronics and Telecommunication, JSPM's Rajarshi Shahu College of Engineering, Tathawade, Pune, Maharashtra, 411033, India

^b Department of Electronics and Telecommunication, MES's College of Engineering, Pune, Maharashtra, 411001, India

^c Department of Electronics and Telecommunication, Dr. D. Y. Patil Institute of Technology, Pimpri, Pune, Maharashtra, 411018, India

ARTICLE INFO

Keywords:
Drought
Satellite images
Preprocessing
Drought indices
Chimp optimization

ABSTRACT

The change in climate and the hot temperature environment increased the risk of drought around the workplace. Predicting and forecasting the drought occurrence is essential for managing water resources and agricultural plans. Therefore, in this study, a novel Chimp-based Wide ResNet Prediction Framework (CWRPF) is designed to predict the drought. The key motive of the presented research is to predict the drought and no drought conditions derived from the satellite images. The satellite images are collected from the Bhuvan site. Initially, the satellite images are noise-filtered. The filtered images are then injected into the feature analysis phase to compute the drought indices of a specific area by the fitness function activated in the framework. After estimating the drought indices, the drought condition was categorized. Finally, the designed system is tested in the MATLAB platform and has gained more significant results by providing a 97.68% accuracy rate, R² as 0.998, and lower RMSE and MAE values of 0.223 and 0.193. The accumulated results are compared with existing techniques to validate the improvement score. The accuracy of the CWRPF is more remarkable than that of other prediction models. Therefore, the system is efficient for drought prediction in satellite images.

1. Introduction

Drought is an extended dry time in the natural climatic cycles, sometimes over months or years (Adar et al., 2022). Based on the form of the drought, it is categorized into four types. They are agricultural, meteorological, socioeconomic, and hydrological droughts. Generally, a meteorological drought is identified as the lack of rainstorms in the region over a long period (Arab et al., 2021). Drought in the specific area is determined by the moisture-less air, no precipitated weather conditions, and increased surrounding temperature, and it varies depending on the location. An agricultural drought arises whenever the watery atmosphere is reduced to a certain level and the ground is affected (Buthelezi et al., 2022). The growth of crops and animals in agricultural land is reduced, and production is concerned. It creates an imbalance in the food chain and affects daily life (Gavrilescu 2021). A hydrological drought is described as the degradation of long-term water sources such as lakes, ponds, rivers, etc.; when the water sources fail to satisfy the demand for economic goods, a socioeconomic drought occurs (Wu et al., 2022). The betterment period of this drought was relatively more extended than that of others. The drought is divided based on the period of precipitation (Adaawen 2021). Drought can affect crop yields and

* Corresponding author.

E-mail addresses: Bdjadhav_entc@jspmrscoe.edu.in (B. D Jadhav), pmghate_entc@jspmrscoe.edu.in (P. Marotrao Ghate), prabhukota1@gmail.com (P.N. Kota), sdchavan73@gmail.com (S.D. Chavan), pbcopade@mescoepune.org (P.B. Chopade).

food chains and shorten the water supply (Javed et al., 2021). Characterizing drought is essential for controlling operations and preparedness for the mitigation plan. The detection of drought is complex due to three reasons (Abdullah et al., 2021). Firstly, the slow development and the end of the onsets are different. Second, drought is universally defined and not structured and disperses over a wide area. The various meteorological parameters like humidity, water evaporation, rainfall, moisture, and temperature help define drought (Danilevskaya et al., 2019).

Severe drought events have left extreme ecosystem destruction and resulted in a low productivity rate (Li et al., 2020). The average yearly rainstorms can measure the intensity of the drought. However, the correct recognition is complex due to the depletion of characteristics such as duration and extent (Abushandi and Al Ajmi, 2022). Therefore, the spatial and temporal patterns should be identified to specify the features. The various indices quantify the occurrence and drought distribution. They are the Standardized Precipitation Index (SPI), Palmer Drought Severity Index (PDSI), Soil Moisture Index (SMI), Standardized Groundwater level Index (SGI), and Standardized Precipitation Evapotranspiration Index (SPEI) (Lee et al., 2020). The data for the unreachable areas on the ground and the wider dimensional area can be obtained through satellite images. Numerous studies have demonstrated drought identification through satellite images (Sultana et al., 2021). A few of the satellite imagery-based indices that are generally applied for drought assessment comprise normalized differences in the Enhanced Vegetation Index (EVI), Normalized Differences Vegetation index (NDVI), Vegetation Health Index (VHI), and Leaf Area Index (LAI). However, numerous drought identification models were designed with detection capability (Mohanasundaram et al., 2023; Jiao et al., 2021). In recent years, many ML techniques have been increased for drought detection. In such methods, the incorrect recognition caused by combined meteorological factors remains a problem (Balti et al., 2020). To cover these problems presented, a new design for drought identification was presented through satellite images.

One of the most serious environmental hazards that impact the growth of socio-economic and the environment is drought. It leads to crop failure, famine, and water shortage. The early and robust prediction of drought will help to mitigate these problems. Therefore a new study is created in this research. The objective of this study is to create a unique method to forecast the drought conditions of the land using satellite images of West Bengal. This research examines how well the deep learning model forecasted the meteorological drought condition and explored the drought prediction variation defined by different index values. The model is created to identify the drought at an early stage for timely mitigation plans. It provides a comprehensive analysis of the wide drought-affected regions. It categorized the mild, moderate, and severe drought. The traditional studies depend on the ground observations which limit the wide coverage and time consuming. The present study accesses Landsat satellite images taken from 2010 to 2014 to predict the drought vulnerability of a large area.

The paper arrangement of the presented article is described as follows: recent drought identification models, their merits, and research gaps were discussed in section 2, the motivation of the present research is explained in section 3, the process of the developed drought prediction model is detailed in section 4, results of the designed model is evaluated in section 4, and section 5 provided the conclusion with future work.

2. Related works

Some recent works of literature related to drought prediction through satellite image processing are described as follows.

Models such as Supporting Vector Machine (SVM) (Zhu et al., 2021), Artificial Neural Network (ANN) (Hassanzadeh et al., 2020), Fuzzy Logic (FL) (Hoque et al., 2021), and different hybrid technologies were used for the prediction of drought. Identifying the drought is mainly aimed at regulating the initial mitigation plans. Previous research has focused on designing detection models using remote sensing data. These models are complicated to utilize because they need decades of weather data (Bandyopadhyay et al., 2020). A detection system to predict drought based on the soil's moisture level was also created (Xu et al., 2020). However, due to the grand scale model, it is complex to create the mitigate plans.

Park et al. (2019) designed a Severe Drought Region Forecast (SDRF) model using the data from remote sensing via Region Forecast (RF). The process of this model is categorized into two parts. Initially, the RF is trained to learn the SMI from the past drought and to compute the Root Mean Square Error (RMSE), determination coefficient (R²), and Mean Absolute Error (MAE). Secondly, the trained function evaluates the SMI for the tested area and the RMSE value for drought prediction. Also studied, the variable parameter originated from the RF. It is easy to understand. If the site has yet to experience drought, the detection is difficult due to learning about past droughts.

Kaur and Sood (2020) introduced the Drought Assessment system based on Deep Learning (DADL) for effective drought detection and control. Here, the data is initially collected by Internet of Things (IoT) sensors and reduces the size of the fog layer. Then, the drought evaluation takes place at the deep learning frameworks. Additionally, the SVR supports drought prediction. The execution time is less due to the reduced data. However, an increase in the time frame of the forecast increases the error rate.

Dikshit et al. (2020) conducted the drought prediction framework with two phases. Initially, the SPEI is evaluated using a climatic dataset. Secondly, the data is trained and tested in the SVM. The testing was executed using statistical terms such as RMSE, MAE, and R² for both periods. The difference between the determined and acquired SPEI values depends on drought categories determined using the ROC and AUC parameters. It contains both classification and regression processes. However, it concerns only short-term drought.

Singh et al. (2021) demonstrated the ANN model for assessing and identifying drought risk. This model was executed based on integrating a few indices, such as PCI, TCI, SCI, and VCI, obtained from the satellite imagery data applied for this study. Here, the results are accurately investigated using the ANN model with agricultural and meteorological drought information. This model gained better accuracy and is helpful to farmers for early drought detection. However, for training, this model requires a lot of data.

To reduce the significant impact of agricultural drought, Yoon et al. (2020) studied drought forecasting based on the Evaporative

Stress Index (ESI). Here, the suitability of the ESI is analyzed through two approaches: qualitative analysis and grid values. Here, the grid values are extracted from the satellite images, and each index is re-framed to identify intense drought. The index with a better reflection of the drought was confirmed. However, it is crucial to know the index's sensitivity to the drought to reduce the error values.

The main contribution of the presented framework is described as follows.

- A novel Chimp-based Wide ResNet Prediction Framework (CWRPF) is designed with various feature parameters.
- The preprocessing phase removes the noise from the input images.
- Moreover, the Chimp fitness function estimated the drought indices in feature analysis.
- Finally, the drought conditions are predicted by the estimated drought indices.
- Subsequently, the performance is validated and compared with other techniques regarding Accuracy, Mean Absolute Error (MAE), Root Mean Square Error (RMSE), and Determination Coefficient (R^2).
- The performances are validated by training and testing the model with the collected satellite image and indices data.

3. System model and problem statement

The precise detection of any natural hazards is a complex procedure. Drought identification is difficult among all environmental disasters because of the lack of a universal definition and the impacts of climate change both spatially and temporally. Various models were investigated to acquire higher results and support us in learning about the different drought conditions and periods. Initially, data were collected and trained on Machine Learning (ML) or Deep Learning (DL) models to analyze various indices. Through the analysis of those indices, the assessment and the prediction of drought are carried out.

However, these models require a larger dataset, and the computation time is more considerable. Also, the prediction accuracy becomes low, resulting in a higher error rate. These limitations have inspired the suggested framework for drought identification using satellite imagery. The same input with the related time scales and the computation time length is critical for exact predictions. Also, suitable preprocessing methods will improve the accuracy of models. So, to enhance the preprocessing and the accurate forecast, the presented model was implemented. The system model architecture with the problem statement is shown in Fig. 1.

4. Proposed CWRPF for drought prediction

A novel CWRPF is proposed to predict the drought condition. This study aims to predict and classify the input satellite images into drought and no drought categories based on the drought indices measures. The proposed technique is helpful for the growth of crops in suitable areas. For the processing of CWRPF, the satellite images with the vegetation index data are collected from the Bhuvan site (<https://bhuvan.nrsc.gov.in/>) and GRACE data. Initially, the images are preprocessed to eliminate the image and data noises, and the features are extracted through the tracking function of the chimp. In the presented model, the extracted features are the values of SMI and ESI. Further, the chimp's fitness function predicts the drought based on the extracted drought indices values. Here, the Chimp-based Wide ResNet is utilized for the feature analysis and estimation of drought indices. The process of the proposed CWRPF is given in Fig. 2.

Moreover, the prediction results are calculated, and the improvement score is computed by comparing it with other prevailing techniques based on drought prediction. The proposed framework analyzes the two features by applying the chimp function. Also, the classification parameters are adjusted by the fitness function for an accurate forecast.

4.1. Study area

The study area focused on implementing this framework is the Purulia district of West Bengal, India. The Purulia district is one of the main drought-prone areas in West Bengal. Here, the maximum temperature ranges from 28°C to 40°C , and the rainfall range is

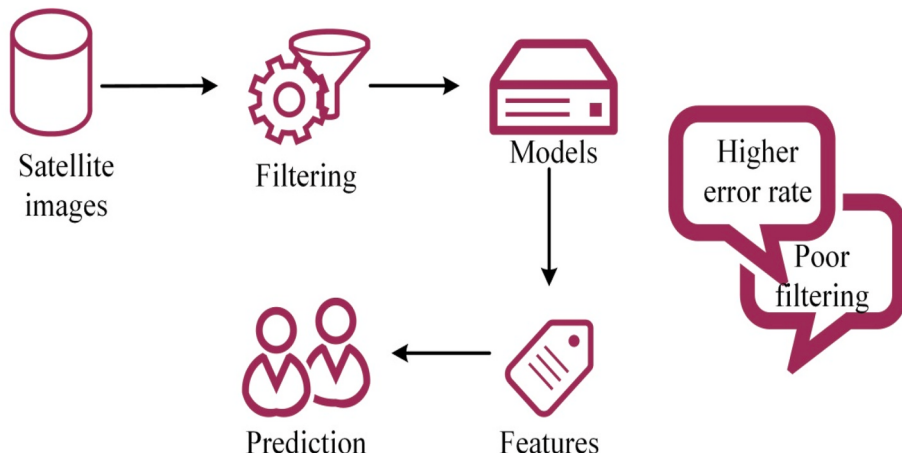


Fig. 1. System architecture with its problems.

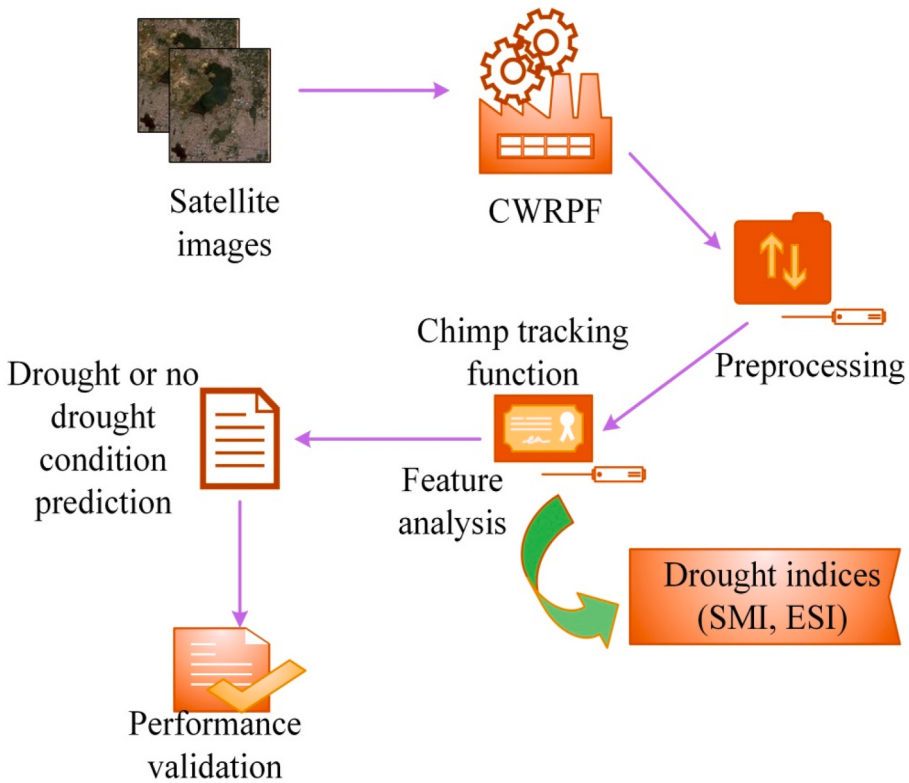


Fig. 2. Proposed CWRPF architecture.

1100–1500 mm.

In India, the eastern part experiences frequent droughts. So, for the present study, West Bengal is selected for the drought assessment. The study area is shown in Fig. 3. In Fig. 3 (A), the West Bengal region is marked as a dark brown shade. In Fig. 3 (B), the area shaded in red is the Purulia district, the chosen study area from West Bengal.

4.2. Design of presented CWRPF layers

The suggested system combines Chimp optimization (Khishe and Mosavi 2020) and Wide ResNet (Song et al., 2021). The residuals are the essential factor in the residual network. So, this framework used wider residual blocks, which comprised more filters at the convolution layer. Enhancing the width of the residual network is computationally efficient for the training process, and in the proposed model, the residual blocks are perfectly stacked to overcome the failures. The Chimp fitness features are activated at the classification layer of the framework to obtain accurate results. The chimp optimization explains the four hunting behaviors of the chimp for the prey. The chimp is divided into four groups for each behavior, and finally, the position of the best chimp is updated depending on the distance to the prey. The developed CWRPF consists of several layers: preprocessing, feature analysis, prediction, and output. Here, the satellite images with drought indices features are collected for training.

$$f(S_i) = \{1, 2, 3, 4, 5 \dots n\} \quad (1)$$

Here, S_i denote the satellite data images. Eqn. (1) processed the training function. Moreover, the CWRPF layers are detailed in Fig. 4.

The noise features from the satellite images can be removed in the preprocessing function of the hidden layer. Subsequently, the presented features were analyzed in the feature analysis process. The drought indices were analyzed. Finally, the drought condition is predicted at the classification layer and presented at the output.

4.2.1. Data preprocessing

The foremost step carried out before the data training is preprocessing. Preprocessing was carried out using the in-depth features of the network. The salt and pepper noise is the most common in computerized satellite images. In this stage, the noise in the collected satellite images is removed through the convolution filters of the designed architecture. Additionally, unwanted and unused data was also released in this phase. Eliminating noise and unwanted data balances the dataset's consistency for easy prediction with great accuracy. The preprocessing function is expressed in Eqn. (2).

$$\Delta_p(S_i) = \sum_n \partial(S_i - a) \quad (2)$$

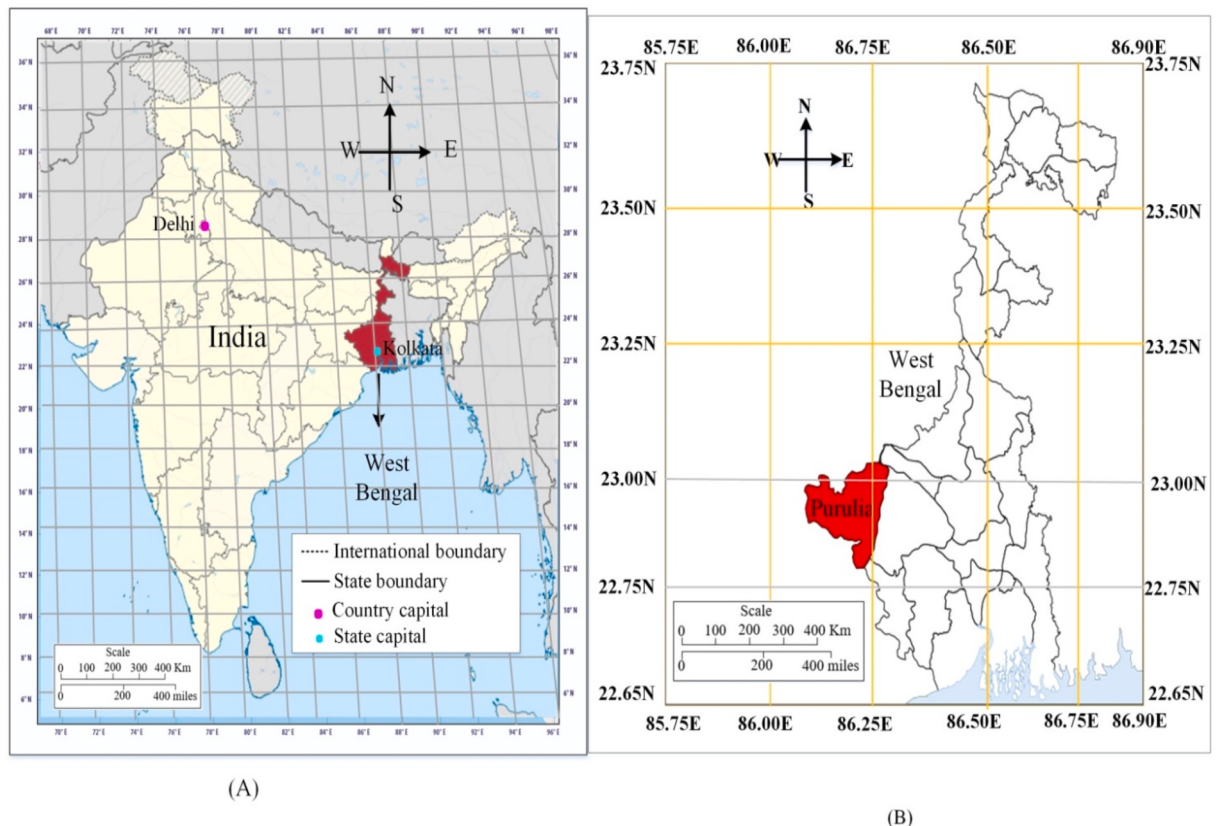


Fig. 3. Study Area (A) India map, (B) West Bengal.

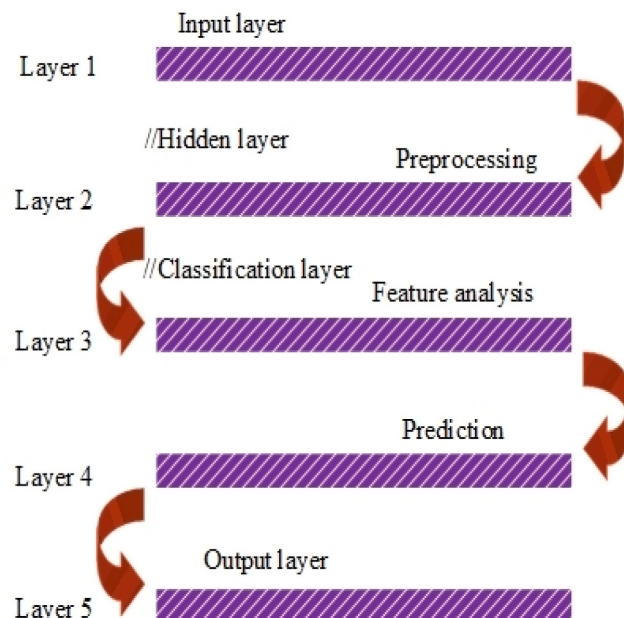


Fig. 4. Layer diagram of CWRPF.

Hence, δ it is determined as the noise tracing parameters, and the preprocessing variable is represented as Δ_p and a represents the noise features. Also, the filtering of images reduces the prediction complexity and the execution time.

4.2.2. Feature analysis

The preprocessed images are then entered into the feature analysis phase. The droughts are identified based on several indices. This framework analyzed indices such as the Soil Moisture Index (SMI) and Evaporative Stress Index (ESI) for drought prediction. The SMI determines the moisture condition of the land at various depths. ESI observes the temperature of the land surface, which is used to estimate water loss. It is more sensitive than other indices. Eqn. (3) analyzed the features.

$$\alpha = t_a [S_i - (s_m, e_s)] \quad (3)$$

Here, α it is represented as the feature extracting variable, t_a is the feature tracing parameter, s_m indicates the SMI, and e_s represents the ESI. Here, the analyzed features are SMI and ESI.

$$x_t = \frac{\alpha}{S_i} \quad (4)$$

Here x_t is the location updating variable taken from chimp fitness and using chimp fitness, using Eqn. (4) the indices such as SMI and ESI are analyzed from the study area.

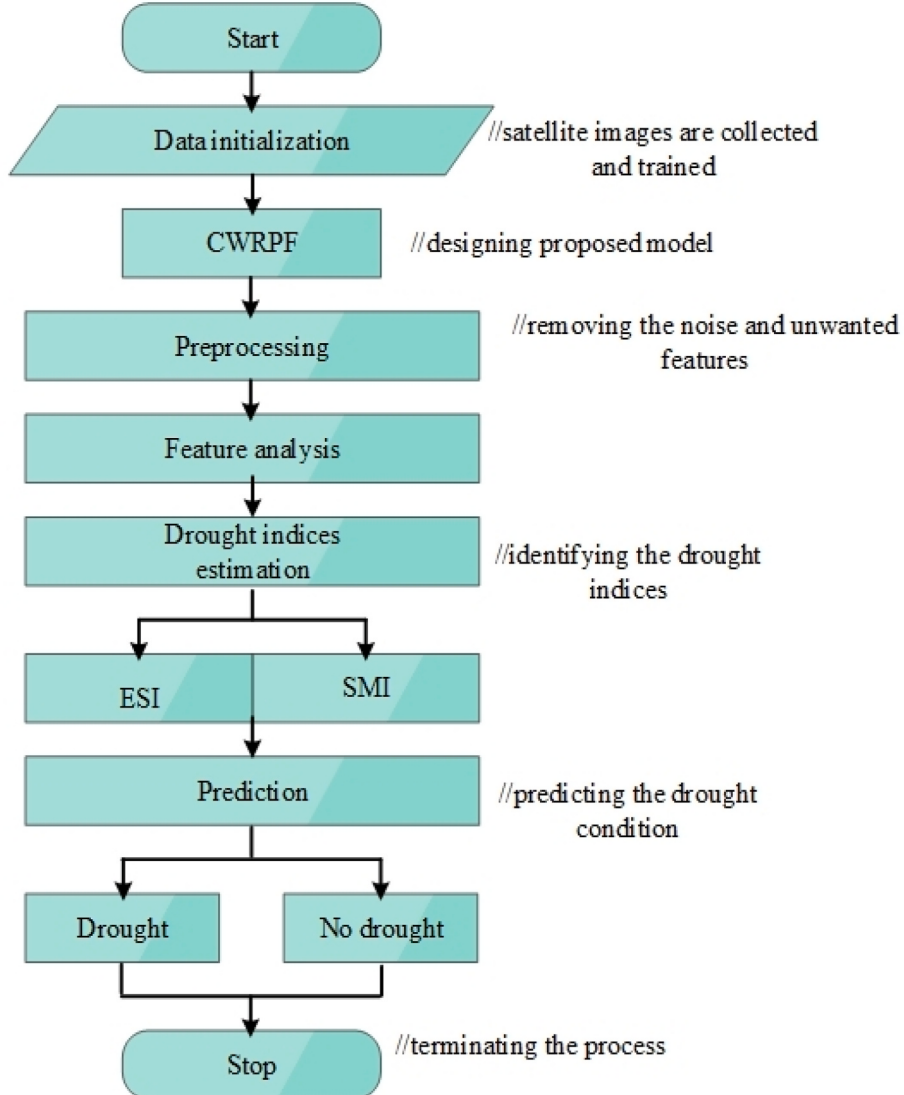


Fig. 5. CWRPF process flowchart.

4.2.3. Prediction

After analyzing the selected drought indices, the area is predicted to be in drought or no drought condition. Here, the drought condition is predicted using the state given in Eqn. (5).

$$\text{prediction} = \begin{cases} \text{if } (x_t \geq 0.5) & \text{no drought} \\ \text{if } (x_t < 0.5) & \text{drought} \end{cases} \quad (5)$$

Here x_t are the analyzed drought indices that range [0, 1]. Thus, the drought condition is predicted from the specific area by examining the index.

The steps and processes presented in the designed model were detailed in Algorithm 1. The MATLAB code was executed based on these step processes, and the results were verified. The algorithm incorporated all mathematical function parameters in the pseudo-code format. These processes are given step by step in algorithm 1.

The satellite images are preprocessed and trained in the system in the training phase to study the specific area's drought features and indices. The preprocessed images are feature-analyzed in the testing phase, and the estimated drought indices use the trained features. By the estimated value of the drought indices, the drought condition of the specific area is categorized as drought or no drought. The prediction process of the designed framework is explained in the flowchart given in Fig. 5.

5. Results and discussion

The suggested framework is executed on the MATLAB platform using satellite imagery. The noise and unwanted data are removed, and the error-free data are obtained for training and further processing. The execution components required for implementing the presented technique are tabulated in Table 1.

5.1. Case study

A case study was conducted to study the operating efficiency of the presented system, and the input pictures considered for the execution were satellite pictures. Moreover, the resultant images gained for preprocessing, feature extraction, and recognition are explained below.

5.1.1. Dataset

The satellite images are collected from the ISRO Bhuvan site from the Landsat 8 satellite. Initially, it is converted into an Environment for Visualizing Image (ENVI) format using R-package, which is suitable for image processing and analysis. To estimate the SMI and the ESI, the Gravity Recovery and Climate Experiment (GRACE) data were utilized. Here, the collected input data is 3460 satellite images of specific places in the Purulia district in West Bengal, India, and GRACE data to train the network to learn the drought indices of the region. Here, 2768 images were taken from the GRACE data, and the remaining 692 images were taken from the Bhuvan site. The study covered the period from 2010 to 2014 with an image resolution of 30m. The frequency range of the satellite images is 0.433–2,300 μm . Among the total input images, 70% (2422 images) are taken for training, 10% (346 images) for validation, and 20% (692 images) for testing. The validation set estimates the network training performance and decides when to stop the training.

5.1.2. Drought identification

The satellite images are required to predict drought conditions. Here, the satellite images of the Purulia district with drought indices are collected and trained. The preprocessing is done to remove the noise features present in the pictures. After, the parts are analyzed to extract the value of indices such as SMI and EVI. From the extracted indices range, the drought condition of a specific area is predicted. In this presented framework, the ESI and SMI measures detected the water features of a particular area in the input satellite images.

The region with low water features was indicated as drought, and the higher water level was detected as a no-drought region. Thus, the designed model classified the drought and no drought satellite images. The prediction and output are shown in Fig. 6. The loss and accuracy graph attained for training and validating the collected data in the MATLAB environment is shown in Fig. 7.

5.1.3. Practical implications

The proposed model identifies the short-term drought condition that human action can easily handle. It helps to identify the area susceptible to drought and to provide mitigation plans to avoid long-term issues. This model is easy to access. It helps with the provision of a rapid supply of water. The developed image processing algorithm supports the decision makers in organizing the appropriate land use planning. Furthermore, the data-driven events are more efficient for drought forecasting for the selected study.

Table 1
Implementation parameters.

Parameters	Description
OS	Windows 10
Platform	MATLAB
Version	R2021a
Data types	Satellite images
Analyzed properties	SMI and ESI

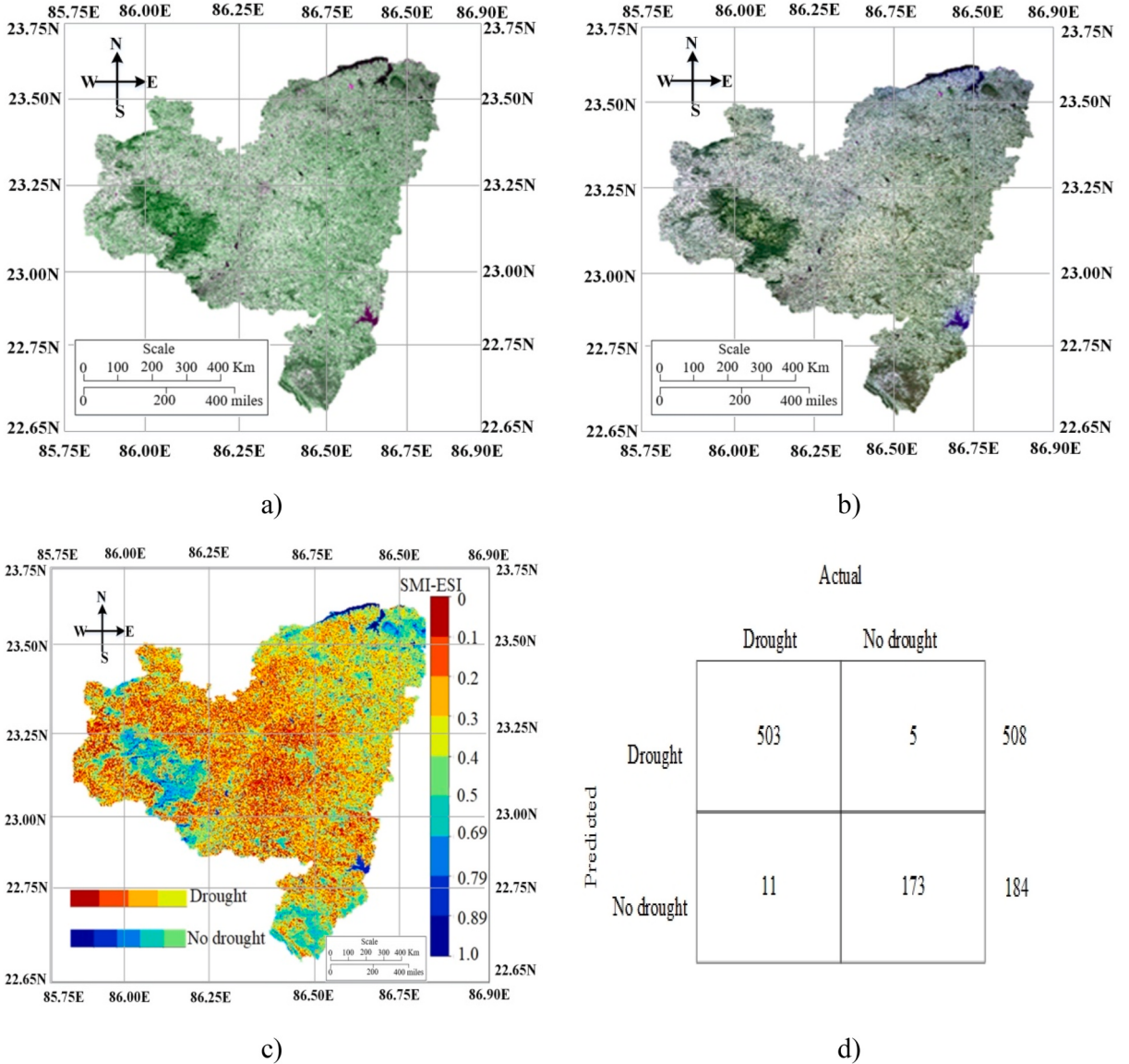


Fig. 6. Drought identification: a) Input image, b) Preprocessing and c) Feature analysis and prediction, d) Confusion matrix.

area. Also, it helps manage water sources in a dry environment.

5.2. Performance analysis

To estimate the efficiency of the presented framework, the resulting values are compared with a few existing techniques such as Combined Functional link Random vector (CFR) (Adnan et al., 2021), M5P Model Tree (MMT) (Pande et al., 2022), Deep Belief network based Long-term Drought Prediction (DBLDP) (Agana and Homaifar 2017) and Hybrid Boosting and Supporting Vector Regression (HBSVR) (Fung et al., 2019) in terms accuracy, RMSE, MAE and R^2 .

5.2.1. Accuracy

One of the critical parameters to find the proposed CWRPF's performance stability is termed accuracy. Here, the accuracy can be validated based on the estimated statistical parameters of the drought indices. In addition, it can be calculated by dividing the predicted results by the total performance. Eqn. (6) can calculate it.

$$\text{Accuracy} = \frac{t_p + t_n}{t_p + t_n + f_p + f_n} \quad (6)$$

Here t_p is a true positive, t_n true negative, f_p false positive and f_n false negative.

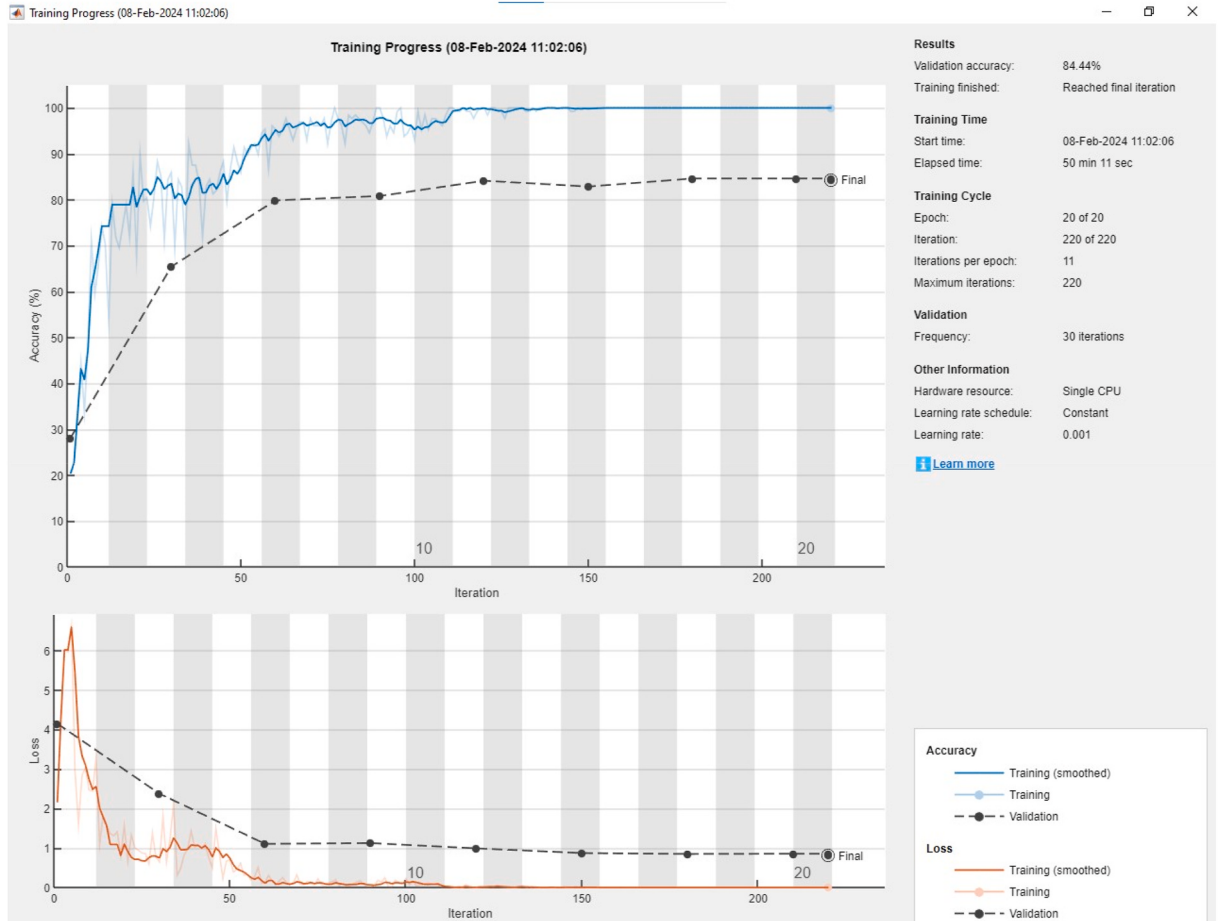


Fig. 7. Accuracy and loss curve.

Here, the presented CWRPF is compared with the existing techniques. The current frameworks, such as CFR, gained an accuracy rate of 92%, MMT obtained 94.3%, DBLDP acquired 95%, and HBSVR gained 91.7% of accuracy. The proposed framework resulted in 97.68% precision, higher than that of the other existing models. In the proposed technique, the activation of the chimp fitness increased the accuracy. The comparison of accuracy with prevailing models is shown in Fig. 8.

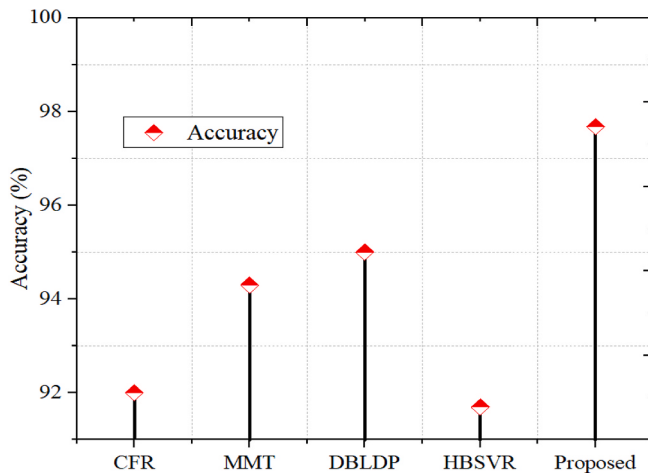


Fig. 8. Accuracy comparison with existing techniques.

5.2.2. Determination coefficient (R^2 or R-square) validation

The R^2 is measured to compute the relationship between the independent and dependent parameters. The statistical measurement validates the difference between the one variable estimated from the difference of another variable when the outcome of the presented framework is obtained. It is determined by the formula expressed in Eqn. (7).

$$R^2 = \left[\frac{\sum_{k=1}^C (v_p - \bar{v}_p)(v_o - \bar{v}_o)}{\sqrt{\sum_{k=1}^C (v_p - \bar{v}_p)^2(v_o - \bar{v}_o)^2}} \right]^2 \quad (7)$$

Here v_p is the predicted value of indices, \bar{v}_p the average expected value, v_o the observed value, and \bar{v}_o the moderate observed value.

The existing models, such as CFR, recorded the R^2 as 0.815, MTT gained 0.728, DBLDP obtained 0.934, and HBSVR gained 0.987 as the R^2 rate. The proposed technique resulted in an R^2 value of 0.998. The CWRPF model system attained the highest R-square value compared to other existing frameworks, and the comparison is shown in Fig. 9. The higher the R^2 value, the more the error value of the prediction model decreases.

5.2.3. MAE and RMSE assessment

MAE and RMSE are computed to study the ability of the proposed CWRPF to calculate drought indices and predict drought conditions. The lower rate of MAE and RMSE indicates a better determination coefficient and prediction results. The root value of the validated MSE can compute the term RMSE. The RMSE calculation is expressed in Eqn. (8).

$$RMSE = \sqrt{\frac{1}{C} \sum_{j=1}^C (v_o - v_p)^2} \quad (8)$$

Here v_p and v_o are the predicted and observed values. It also C denotes the observation counts. RMSE is one of the standard deviation statistics parameters.

The model CFR has recorded the RMSE at 0.489. The MMT scheme has obtained an RMSE score of 0.551; the DBLDP replica has acquired an RMSE value of 0.4572. Moreover, the HBSVR strategy has earned an RMSE of 0.249. Finally, the presented CWRPF has caught an RMSE of 0.223. Compared to other prevailing frameworks, the proposed framework achieved a low RMSE rate, which shows the enhanced performance of the presented framework. These results are discussed in Fig. 10.

In addition, the MAE can be calculated by the expression given in Eqn. (9).

$$MAE = \frac{|(l_o - l_p)|}{C_n} \quad (9)$$

Here, the actual value is denoted as l_o , l_p the predicted value and C_n is the observation number. The MAE has calculated the difference between the actual value and the estimated.

The model CFR has gained 0.337 of MAE. The MMT model has obtained an MAE of 0.388; the approach DBLDP has made an MAE of 0.285. Also, the HBSVR strategy has earned the MAE value of 0.205. The presented CWRPF has gained an MAE of 0.193. Compared to other prevailing frameworks, the proposed framework achieved the minimum MAE rate, which shows the enhanced performance of the presented framework. The comparisons of these statistics are shown in Fig. 11. The overall comparisons are tabulated in Table 2.

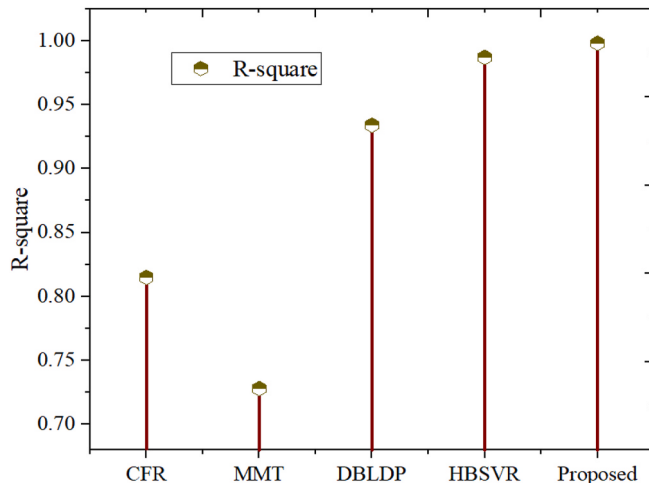


Fig. 9. Determination coefficient comparison with existing models.

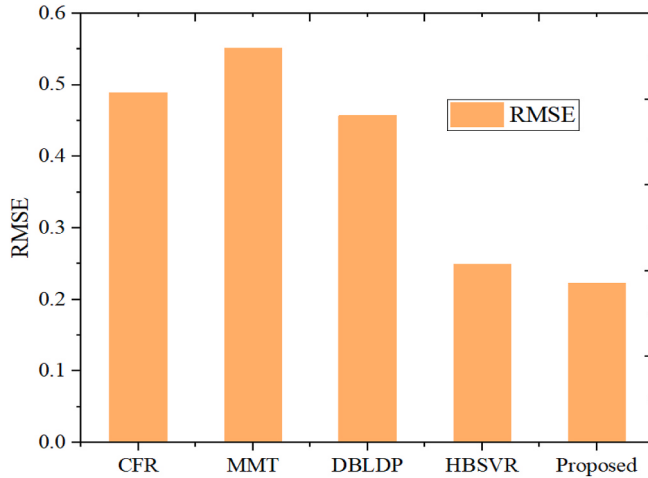


Fig. 10. RMSE comparison with different methods.

Additionally, the efficiency of the proposed approach is analyzed by classification metrics such as specificity, recall, and f-score. Specificity identifies the correctly predicted no drought condition rate, recall validates the rate correctly recognized drought condition images, and f1-score is the mean value of the above two metrics. The comparisons of these metrics are detailed in Fig. 12.

In this comparison, it is clear that the proposed method validated the higher values for the performance metrics such as precision, recall, and f1-score. It scored a precision of 99%, recall of 97.8%, and f-score of 98.4%. The other prevailing models attained lower values than the proposed method for the three considered classification metrics. Among those models, the HBSVR system performs poorly for the drought classification from the satellite images. Therefore, the designed system correctly predicted the drought condition of more tested satellite images. The designed CWRPF system is more robust for the prediction of drought than the previous method. The model integrated the wide Resnet and Chimp optimization components, which is shown as the novelty of this research. The designed model comprises a larger number of channels than any other network to capture all the complex features from the input data. The Chimp optimization optimized the hyperparameters for better predictive learning which can improve the performance of the model for the drought prediction than any other methods.

5.3. Discussion

The suggested framework has achieved the finest recognition outcome from the performance assessment, which is relatively better than the previous studies. Hence, these performance improvements are verified by performing the comparative studies in the last section. The error rate is also validated for the present model.

Compared to the existing system, the presented model achieves a higher accuracy and R^2 and low MAE and RMSE scores. The overall performance of both datasets of the proposed model is listed in Table 3. The lower value of RMSE and MAE error metrics shows the accurate calculation of the indices. Using ESI and SMI in the proposed prediction structure is advantageous for mid and short-term drought identification. Therefore, this system is more effective for drought identification. The training function and convergence of the optimal solution are faster in the network. Accordingly, the system can process a large number of data. Also, the comprehensive layers of the network increased the prediction accuracy. The ability of the drought prediction is increased by the data noise elimination at the preprocessing phase of the designed model. The designed approach can also be used with other datasets to improve various drought identifications. The model provides timely and accurate predictions, which are helpful for mitigating drought-related impacts. The model can be trained on data from diverse regions and environmental conditions, making it generalizable to different landscapes and drought characteristics. The hyperparameter tuning of Wide ResNet architecture using the Chimp fitness process further improved its accuracy and performance. However, when the accuracy increases, the cost of networks also increases due to the widening of the framework. Sometimes, the optimization function in the proposed network may fall into a local optimum problem. The suggested model provided the higher efficient results for drought prediction. The short-term drought states that can be managed by human activity are identified through the suggested model. Also, to prevent long-term problems, it helps to identify the areas that are vulnerable to drought for establishing mitigation plans. The model is simple to access. It helps to facilitate the delivery of an immediate supply of water. The decision-makers are assisted in planning the proper land use by the created image processing algorithm. Additionally, for the chosen study area, data-driven events are more effective in predicting droughts. It also aids in the management of water supplies in arid environments.

The satellite images of the different regions differ in spectral bands and resolution. Also, environmental variations occurred in the different drought regions. However, the presented model provides the same results for the different settings. The fine-tuning mechanism of the chimp optimization in the designed network helps the prediction system to adapt to environmental characteristics and other settings.

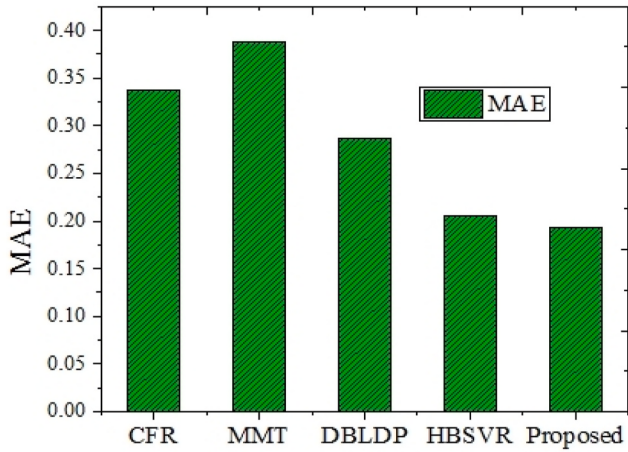


Fig. 11. MAE comparison with existing models.

Table 2
Overall performance comparisons.

Metrics	CFR	MMT	DBLDP	HBSVR	Proposed
Accuracy (%)	92	94.3	95	91.7	97.68
RMSE	0.489	0.551	0.4572	0.249	0.223
MAE	0.337	0.388	0.285	0.205	0.193
R ²	0.815	0.782	0.934	0.987	0.998
Error (%)	8	5.7	5	8.3	0.2
Recall (%)	92.8	95	95.6	92	97.8
Precision (%)	92.9	94.8	95.7	91.8	99
F1-score (%)	92.86	94.7	95.9	91.89	98.4

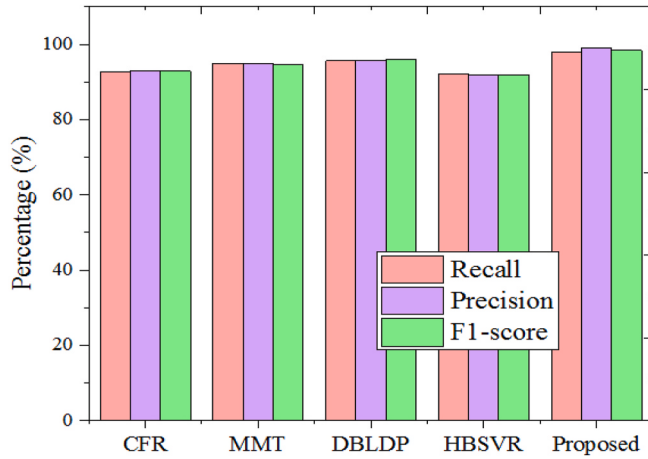


Fig. 12. Recall, precision, and f1-score comparison.

5.3.1. Limitations and future work

The limitations in the designed prediction model are local minima, prone to overfitting and memory-intensive networks, and limited in predicting the various drought categories that include many parameters. Additionally, acquiring high-resolution satellite imagery can be expensive frequently and impractical. At the same time, the limited-resolution images can lead to missing crucial information about drought development and hinder the model's ability. Validating and calibrating drought assessment models often require ground truth data, such as field observations and soil moisture measurements. However, acquiring comprehensive and reliable ground truth data can be expensive and time-consuming. In the future, other effective indices can improve drought identification, and fine-tuning strategies with efficient optimization will enhance the results. Also, the techniques can be adapted to other remote sensing applications such as land cover and crop yield prediction.

Table 3

Overall performance of CWRPF.

Parameters	Values
Accuracy	97.68%
MAE	0.193
RMSE	0.223
R ²	0.998
Error rate (loss)	0.2
Recall	97.8%
Precision	99%
F1-score	98.4%

6. Conclusion

This research proposed a novel CWRPF system using satellite images to predict drought in a specific area. The satellite images of the study region with the drought indices data are collected and preprocessed to remove the noise features and unwanted data. Furthermore, features such as SMI and ESI are extracted from the images using the Chimp function. Subsequently, from the extracted indices, the drought condition of the specific area is predicted and categorized using the Chimp fitness function. The model categorizes the area as drought and no drought conditions. The designed CWRPF is executed in the MATLAB tool to validate its robustness. The validated outcomes are compared with existing techniques, and performance improvement is noted. The accuracy result of the CWRPF system is 97.68%, which is an increase of about 2% from the available methods. The values of a few more statistical terms, such as MAE, RMSE, and R², are 0.193, 0.223, and 0.998, which is more efficient than other existing approaches. Also, the recall, precision, and f1-score measures are valued at 97.8%, 99%, and 98.4%, respectively. These parameters proved the working efficiency of the system.

Funding

This research received no specific grant from funding agencies in the public, commercial, or not-for-profit sectors.

CRediT authorship contribution statement

Bhagvat D Jadhav: Writing – review & editing, Data curation, Conceptualization. **Pravin Marotrao Ghate:** Writing – review & editing, Data curation, Conceptualization. **Prabhakar Narasappa Kota:** Writing – review & editing, Data curation, Conceptualization. **Shankar Dattatray Chavan:** Writing – review & editing, Data curation, Conceptualization. **Pravin Balaso Chopade:** Writing – review & editing, Data curation, Conceptualization.

Declaration of competing interest

Authors declare that they have no conflict of interest.

Data availability

No data was used for the research described in the article.

Acknowledgment

None.

Appendix

Algorithm: 1. BUFPS

Algorithm: 1 BUFPS

```

start
{
    int $S_i$ ;
    // initialization of data

    Preprocessing ()
    {
        int  $\Delta_p, \partial, a$ 
        //initializing preprocessing variable
        filtering →  $\partial(S_i) = noise free data$ 
        //noise features are removed
    }

    Feature analysis ()
    {
        int  $\alpha, t_\alpha, s_m, e_s, \beta$       // initialization of feature analysis variables
         $\alpha \rightarrow t_\alpha(s_m, e_s)$ 

         $x_t \rightarrow \alpha / S_i$ 
        //The drought indices were extracted.
    }

    Prediction ()
    {
        if( $x_t \geq 0.5$ )
        {
            No drought
        }
        else
        {
            Drought
        }
        // hence, drought condition is predicted
    }

    Drought conditions in a specific region
}

Stop

```

References

- Abdullah, M.F., Siraj, S., Hodgett, R.E., 2021. An overview of multi-criteria decision analysis (MCDA) application in managing water-related disaster events: analyzing 20 years of literature for flood and drought events. *Water* 13 (10), 1358. <https://doi.org/10.3390/w13101358>.
- Abushandi, E., Al Ajmi, M., 2022. Assessment of hydrological extremes for arid catchments: a case study in wadi Al Jizzi, north-West Oman. *Sustainability* 14 (21), 14028. <https://doi.org/10.3390/su142114028>.
- Adaawen, S., 2021. Understanding climate change and drought perceptions, impact and responses in the rural Savannah, West Africa. *Atmosphere* 12 (5), 594. <https://doi.org/10.3390/atmos12050594>.
- Adar, S., Sternberg, M., Paz-Kagan, T., Henkin, Z., Dovrat, G., Zaady, E., Argaman, E., 2022. Estimation of aboveground biomass production using an unmanned aerial vehicle (UAV) and VENµS satellite imagery in Mediterranean and semiarid rangelands. *Remote Sens. Appl.: Soc. Environ.* 26, 100753 <https://doi.org/10.1016/j.rsase.2022.100753>.
- Adnan, R.M., Mostafa, R.R., Islam, A.R., Gorgij, A.D., Kuriqi, A., Kisi, O., 2021. Improving drought modeling using hybrid random vector functional link methods. *Water* 13 (23), 3379. <https://doi.org/10.3390/w13233379>.
- Agana, N.A., Homaifar, A., 2017. A deep learning-based approach for long-term drought prediction. In: SoutheastCon 2017. IEEE, pp. 1–8. <https://doi.org/10.1109/SECON.2017.7925314>.
- Arab, S.T., Noguchi, R., Matsushita, S., Ahamed, T., 2021. Prediction of grape yields from time-series vegetation indices using satellite remote sensing and a machine-learning approach. *Remote Sens. Appl.: Soc. Environ.* 22, 100485 <https://doi.org/10.1016/j.rsase.2021.100485>.
- Balti, H., Abbes, A.B., Mellouli, N., Farah, I.R., Sang, Y., Lamolle, M., 2020. A review of drought monitoring with big data: issues, methods, challenges, and research directions. *Ecol. Inf.* 60, 101136 <https://doi.org/10.1016/j.ecoinf.2020.101136>.
- Bandyopadhyay, N., Bhuiyan, C., Saha, A.K., 2020. Drought mitigation: critical analysis and proposal for a new drought policy with special reference to Gujarat (India). *Progress in Disaster Science* 5, 100049. <https://doi.org/10.1016/j.pdisas.2019.100049>.
- Buthelezi, M.N.M., Lottering, R.T., Hlatshwayo, S.T., Peerbhoy, K.Y., 2022. Localizing the analysis of drought impacts on KwaZulu-Natal's commercial forests. *Remote Sens. Appl.: Soc. Environ.* 28, 100849 <https://doi.org/10.1016/j.rsase.2022.100849>.
- Danilevskaya, O.N., Yu, G., Meng, X., Xu, J., Stephenson, E., Estrada, S., Chilakamarri, S., Zastrow-Hayes, G., Thatcher, S., 2019. Developmental and transcriptional responses of maize to drought stress under field conditions. *Plant Direct* 3 (5), e00129. <https://doi.org/10.1002/pld3.129>.
- Dikshit, A., Pradhan, B., Alamri, A.M., 2020. Short-term spatio-temporal drought forecasting using random forests model at New South Wales, Australia. *Appl. Sci.* 10 (12), 4254. <https://doi.org/10.3390/app10124254>.
- Fung, K.F., Huang, Y.F., Koo, C.H., 2019. Coupling fuzzy-SVR and boosting-SVR models with wavelet decomposition for meteorological drought prediction. *Environ. Earth Sci.* 78, 1–8. <https://doi.org/10.1007/s12665-019-8700-7>.
- Gavrilescu, M., 2021. Water, soil, and plant interactions in a threatened environment. *Water* 13 (19), 2746. <https://doi.org/10.3390/w13192746>.
- Hassanzadeh, Y., Ghazvinian, M., Abdi, A., Baharvand, S., Jozaghi, A., 2020. Prediction of short and long-term droughts using artificial neural networks and hydro-meteorological variables. *arXiv preprint arXiv:2006.02581*. <https://doi.org/10.48550/arXiv.2006.02581>.
- Hoque, M.A., Pradhan, B., Ahmed, N., Sohel, M.S., 2021. Agricultural drought risk assessment of Northern New South Wales, Australia, using geospatial techniques. *Sci. Total Environ.* 756, 143600 <https://doi.org/10.1016/j.scitotenv.2020.143600>.
- Javed, T., Zhang, J., Bhattarai, N., Sha, Z., Rashid, S., Yun, B., Ahmad, S., Henchiri, M., Kamran, M., 2021. Drought characterization across agricultural regions of China using standardized precipitation and vegetation water supply indices. *J. Clean. Prod.* 313, 127866 <https://doi.org/10.1016/j.jclepro.2021.127866>.
- Jiao, W., Wang, L., McCabe, M.F., 2021. Multi-sensor remote sensing for drought characterization: current status, opportunities and a roadmap for the future. *Remote Sens. Environ.* 256, 112313 <https://doi.org/10.1016/j.rse.2021.112313>.
- Kaur, A., Sood, S.K., 2020. Deep learning-based drought assessment and prediction framework. *Ecol. Inf.* 57, 101067 <https://doi.org/10.1016/j.ecoinf.2020.101067>.
- Khishe, M., Mosavi, M.R., 2020. Chimp optimization algorithm. *Expert Syst. Appl.* 149, 113338 <https://doi.org/10.1016/j.eswa.2020.113338>.
- Lee, H.J., Nam, W.H., Yoon, D.H., Hong, E.M., Kim, T., Park, J.H., Kim, D.E., 2020. Percentile approach of drought severity classification in Evaporative Stress Index for South Korea. *Journal of the Korean Society of Agricultural Engineers* 62 (2), 63–73. <https://doi.org/10.5389/KSAE.2020.62.2.063>.
- Li, J., Wang, Z., Lai, C., 2020. Severe drought events inducing large decrease of net primary productivity in mainland China during 1982–2015. *Sci. Total Environ.* 703, 135541 <https://doi.org/10.1016/j.scitotenv.2019.135541>.
- Mohanasundaram, S., Baghel, T., Udmale, P., Shrestha, S., 2023. Reconstructing NDVI and land surface temperature for cloud cover pixels of Landsat-8 images for assessing vegetation health index in the Northeast region of Thailand. *Environ. Monit. Assess.* 195 (1), 211. <https://doi.org/10.1007/s10661-022-10802-5>.
- Pande, C.B., Al-Ansari, N., Kushwaha, N.L., Srivastava, A., Noor, R., Kumar, M., Moharir, K.N., Elbeltagi, A., 2022. Forecasting of SPI and meteorological drought based on the artificial neural network and M5P model tree. *Land* 11 (11), 2040. <https://doi.org/10.3390/land11112040>.
- Park, H., Kim, K., Lee, D.K., 2019. Prediction of severe drought area based on random forest: using satellite image and topography data. *Water* 11 (4), 705. <https://doi.org/10.3390/w11040705>.
- Singh, T.P., Nanditham, P., Kumbhar, V., Das, S., Barne, P., 2021. Drought risk assessment and prediction using artificial intelligence over the southern Maharashtra state of India. *Model. Earth Syst. Environ.* 7, 2005–2013. <https://doi.org/10.1007/s40808-020-00947-y>.
- Song, M., Mallol-Ragolta, A., Parada-Cabaleiro, E., Yang, Z., Liu, S., Ren, Z., Zhao, Z., Schuller, B.W., 2021. Frustration recognition from speech during game interaction using wide residual networks. *Virtual Real. Intell. Hardw.* 3 (1), 76–86. <https://doi.org/10.1016/j.vrih.2020.10.004>.
- Sultana, M.S., Gazi, M.Y., Mia, M.B., 2021. Multiple indices-based agricultural drought assessment in the northwestern part of Bangladesh using geospatial techniques. *Environmental Challenges* 4, 100120. <https://doi.org/10.1016/j.envc.2021.100120>.
- Wu, J., Yao, H., Yuan, X., Lin, B., 2022. Dissolved organic carbon response to hydrological drought characteristics: based on long-term measurements of headwater streams. *Water Res.* 215, 118252 <https://doi.org/10.1016/j.watres.2022.118252>.
- Xu, L., Abbaszadeh, P., Moradkhani, H., Chen, N., Zhang, X., 2020. Continental drought monitoring using satellite soil moisture, data assimilation, and an integrated drought index. *Remote Sens. Environ.* 250, 112028 <https://doi.org/10.1016/j.rse.2020.112028>.
- Yoon, D.H., Nam, W.H., Lee, H.J., Hong, E.M., Feng, S., Wardlow, B.D., Tadesse, T., Svoboda, M.D., Hayes, M.J., Kim, D.E., 2020. Agricultural drought assessment in East Asia using satellite-based indices. *Rem. Sens.* 12 (3), 444. <https://doi.org/10.3390/rs12030444>.
- Zhu, Q., Luo, Y., Zhou, D., Xu, Y.P., Wang, G., Tian, Y., 2021. Drought prediction using in situ and remote sensing products with SVM over the Xiang River Basin, China. *Nat. Hazards* 105, 2161–2185. <https://doi.org/10.1007/s11069-020-04394-x>.